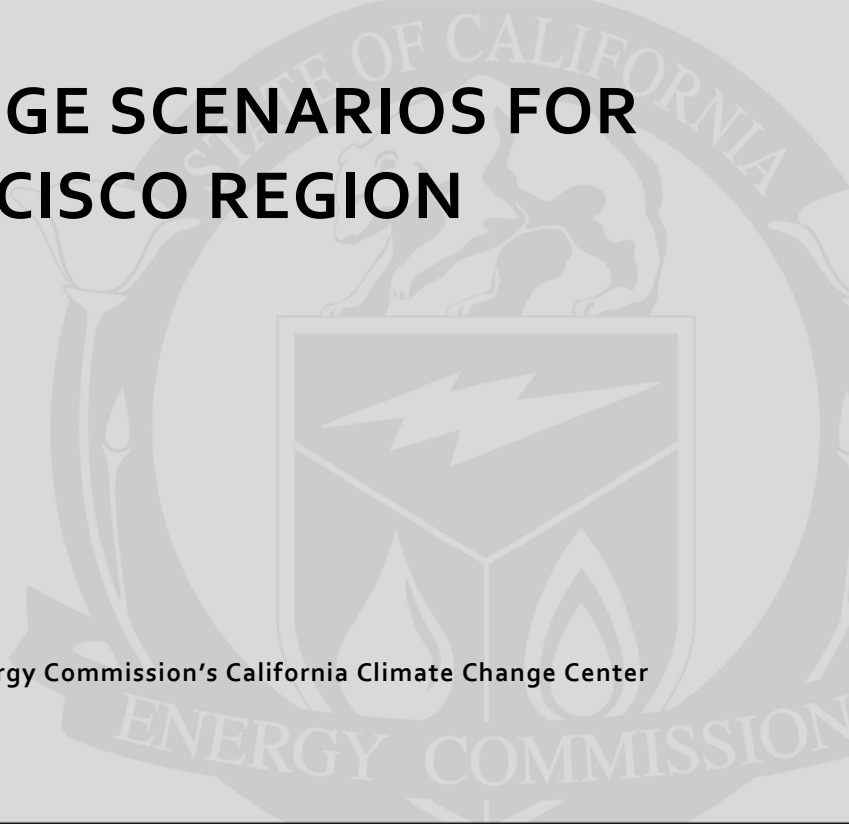


Public Interest Energy Research (PIER) Program White Paper

CLIMATE CHANGE SCENARIOS FOR THE SAN FRANCISCO REGION



A White Paper from the California Energy Commission's California Climate Change Center

Prepared for: California Energy Commission

Prepared by: Scripps Institution of Oceanography, University of California San Diego

JULY 2012

CEC-500-2012-042

Dan Cayan
Mary Tyree
Sam Iacobellis

Scripps Institution of Oceanography
University of California, San Diego



DISCLAIMER

This paper was prepared as the result of work sponsored by the California Energy Commission. It does not necessarily represent the views of the Energy Commission, its employees or the State of California. The Energy Commission, the State of California, its employees, contractors and subcontractors make no warrant, express or implied, and assume no legal liability for the information in this paper; nor does any party represent that the uses of this information will not infringe upon privately owned rights. This paper has not been approved or disapproved by the California Energy Commission nor has the California Energy Commission passed upon the accuracy or adequacy of the information in this paper.

ACKNOWLEDGEMENTS

Support for Dan Cayan, Hugo Hidalgo, Mary Tyree, and Sam Iacobellis was provided by the State of California through the California Energy Commission's Public Interest Energy Research (PIER) Program. Dan Cayan and Mary Tyree were also supported by the National Oceanic and Atmospheric Administration's Regional Integrated Sciences and Assessments (RISA) Program through the California Nevada Applications Program. Thanks to Ed Maurer, Tapash Das, Michael Dettinger, and David Pierce for useful discussion and downscaling information. For global climate model simulations, the authors acknowledge the modeling groups, the Program for Climate Model Diagnosis and Intercomparison (PCMDI) and the World Climate Research Programme's (WCRP's) Working Group on Coupled Modelling (WGCM), for their roles in making available the WCRP CMIP3 multi-model dataset. Support of this dataset is provided by the Office of Science, U.S. Department of Energy.

PREFACE

The California Energy Commission's Public Interest Energy Research (PIER) Program supports public interest energy research and development that will help improve the quality of life in California by bringing environmentally safe, affordable, and reliable energy services and products to the marketplace.

The PIER Program conducts public interest research, development, and demonstration (RD&D) projects to benefit California. The PIER Program strives to conduct the most promising public interest energy research by partnering with RD&D entities, including individuals, businesses, utilities, and public or private research institutions.

PIER funding efforts are focused on the following RD&D program areas:

- Buildings End-Use Energy Efficiency
- Energy Innovations Small Grants
- Energy-Related Environmental Research
- Energy Systems Integration
- Environmentally Preferred Advanced Generation
- Industrial/Agricultural/Water End-Use Energy Efficiency
- Renewable Energy Technologies
- Transportation

In 2003, the California Energy Commission's PIER Program established the California Climate Change Center to document climate change research relevant to the states. This center is a virtual organization with core research activities at Scripps Institution of Oceanography and the University of California, Berkeley, complemented by efforts at other research institutions.

For more information on the PIER Program, please visit the Energy Commission's website <http://www.energy.ca.gov/research/index.html> or contact the Energy Commission at (916) 327-1551.

ABSTRACT

Climate model simulations were used to investigate possible changes in regional climate over California. To accomplish this, the model simulations were downscaled from the coarse global climate model resolution (usually 150 kilometers [km] or greater horizontal grid spacing) to about 12 km horizontal grid spacing over the California region, using statistical techniques. The global model output was used in a statistical modeling scheme to produce sea-level projections for selected California coastal sites. Six global climate models and two greenhouse emissions scenarios, the medium-high emissions Special Report on Emissions Scenarios (SRES) A2 and the lower emissions SRES B1 were considered. By the end of the twenty-first century, the envelope of warming in the models projections, as an annual average, ranges from about 2°C to 6°C (about 3.5 °F to 11°F). On average, mean annual temperature of the A2 scenarios is about 1.5°C (about 3°F) greater than that of the B1 scenario. There is greater warming in summer than in winter. All simulations indicate that hot daytime and nighttime temperatures (heat waves) increase in frequency, magnitude, and duration from the historical period and during the projected period through the first half of the twenty-first century. Projected precipitation is marked by considerable variability between years and decades. In the southern half of California, the models show a decline in annual precipitation. Sea level, at hourly intervals for the historical through the projected twenty-first century, is estimated for selected tide gage sites along the California coast, with rises in the sample of simulations considered here ranging from 27 to 48 centimeters (cm) (11 to 19 in) over historical levels by 2050, and ranging from 77 cm to 140 cm (30 to 55 in) over historical levels by 2100. The rise of mean sea level would provoke an increase in extreme events, as gaged by exceedances above a relatively high or rare historical threshold. Such events become much more frequent and have longer durations than has been seen historically.

Keywords: California, climate change, climate warming, heat waves, sea level rise, downscaled climate simulations

Please use the following citation for this paper:

Cayan, Dan, Mary Tyree, and Sam Iacobellis (Scripps Institution of Oceanography, University of California, San Diego) 2012. *Climate Change Scenarios for the San Francisco Region*. California Energy Commission. Publication number: CEC-500-2012-042.

TABLE OF CONTENTS

Acknowledgements	i
PREFACE	ii
ABSTRACT	iii
TABLE OF CONTENTS	iv
List of Figures	iv
Section 1: Climate Scenarios	1
Section 2: Warming	4
Section 3: Precipitation	8
Section 4: Sea-Level Rise	10
References	13
Glossary	15

LIST OF FIGURES

Figure 1: Observed and Projected Carbon Emissions and Annual Global Atmospheric Carbon Dioxide (CO ₂) Concentration. Emissions (GtC; gigatons of carbon; 1 GtC corresponds to ~3.67 Gt CO ₂) are shown by bars and dots, according to the scale on the right-hand vertical axis. Recent emissions estimates for 2000–2010 are shown by black dots (Carbon Dioxide Information Analysis Center, CDIAC). Historical (observed) emissions are from fossil-fuel burning, cement manufacture, and gas flaring. Carbon dioxide emissions are shown for historical observations (blue bars) and projected periods for B1 (brown bars) and A2 (red bars) emissions scenarios. The annual global atmospheric CO ₂ concentration (in parts per million by volume, ppmv) is shown for the period of observations from 1961 to 2000 (blue line), and for the twenty-first century under two emission scenarios: B1 (brown line) and A2 (red line).	2
Figure 2: The San Francisco Bay Region, with 12 km Downscaled Grid Superimposed. Black dots show the coast-inland transect, and the large black dot indicates the East Bay grid cell that is used in some of the analyses.	3
Figure 3: Annual Temperature (°C left; °F right) Simulated for Historical and Future Periods for the East Bay Grid Cell Using BCS D Downscaling of Six GCMs (CNRM CM3, GFDL CM2.1, MIROC3.2med, MPI ECHAM5, NCAR CCSM3, and NCAR PCM1). Thin grey lines show simulated historical values (1950–1999). Thin blue and red lines show values from B1 and A2 simulations (2000–2099). Thick lines show 11-year running mean smoothed median of historical (black), B1 (blue), and A2 (red) simulations. Horizontal black line shows average of the six GCM’s over the historical (1961–1990) period.	5
Figure 4: Monthly BCS D Simulated Temperature Changes (°C left; °F right) for the East Bay Grid Cell for Six GCMs. Changes (from 1961–1990) are shown for three time periods: early	

century (2005–2034; left), mid-century (2035–2064; middle) and late century (2070–2099; right). Changes are shown in each panel for January (left) to December (right). Black and red symbols show changes for B1 and A2 emission scenarios, respectively. Black (dashed; B1) and red (solid; A2) lines show the median value for each of the six models. GCMs used are those listed in Figure 3. 5

Figure 5: July–September BCSD Surface Air Temperature Changes (°C left; °F right) Over the Coast-to-Inland Transect (see Figure 1). Changes (from 1961–1990) are shown for three time periods: early century (2005–2034; left), mid-century (2035–2064; middle) and late century (2070–2099; right). Changes are shown in each panel over the transect line from west (right) to east (left). Black and red symbols show changes for B1 and A2 emission scenarios, respectively. Black (dashed; B1) and red (solid; A2) lines show the median value for the six models. GCMs used are those listed in Figure 3. 6

Figure 6: Number of Days (n), April–October, When Maximum Temperature (Tmax) Exceeds the 98th Percentile Historical (1961–1990) Level of 28°C (82.4°F) for the East Bay Grid Cell from Four Bias-Corrected/Constructed Analogs (BCCA) Downscaled GCMs. Brown carrots and red dots represent the B1 and A2 emission scenarios, respectively. Thick brown (B1) and red (A2) lines show the median value from the four simulations. 7

Figure 7: Simulated Annual Precipitation (cm right; inches left) at an East Bay Grid Cell from Six GCMs for Historical and Projected Twenty-First Century B1 and A2 Emission Scenarios. The thin black line shows the individual GCM precipitation simulated for 1950–1999. Thin green lines and brown lines show values from B1 and A2 simulations, respectively. Thick lines show 11-year running mean smoothed median of the six historical (black), B1 (green), and A2 (brown) simulations. The GCMs used are those listed in Figure 3. 8

Figure 8: Precipitation Changes (cm right; inches left) for Each Month of the Year, from Six GCMs for the East Bay Grid Cell. Changes (from 1961–1990) are shown for three time periods: early century (2005–2034; left), mid-century (2035–2064; middle) and late century (2070–2099; right). Changes are shown in each panel for January (left) to December (right). Black and red symbols show changes for B1 and A2 emission scenarios, respectively. Black (dashed; B1) and red (solid; A2) lines show the median value for the six models. The GCMs used are those listed in Figure 3. 9

Figure 9: Sea Level (cm) Projections Using the Vermeer and Rahmstorf (2009) Semi-Empirical Scheme. The Vermeer and Rahmstorf (2009) scheme is developed to estimate global mean sea level, but there is general agreement between estimated global sea level and the multi-decade trend of historical observations along the California coast from San Francisco southward to San Diego. The thin black line indicates mean sea level for 2000. Grey lines show global sea-level estimates during the period before 2000 (historical simulation). Sea-level estimates for 2000–2100 are shown using projections from two emissions scenarios: A2 (red) and B1 (blue). Over the twentieth century, sea-level records along the California coast have quite closely mirrored the global rate of sea-level rise. The GCMs used are those listed in Figure 3. 11

Figure 10: Sea-Level Rise and Hours of Extreme Sea Level Projected for San Francisco. The figure shows the annual sea level (cm; black line) and total hours above the historical 99.99th percentile sea level (blue bars) from observations and from sea-level hourly model computations using the GFDL CM2.1 simulation for the A2 emissions scenario as a

representative example. The average number of hours which the projected sea level was found to exceed the historical 99.99th percentile are shown in red for the periods 2005–2034, 2035–2064, and 2070–2099. The projected sea-level rise (secular trend) is based on the GFDL model air temperature and the Vermeer and Rahmstorf 2009 sea-level rise scheme. 12

Section 1: Climate Scenarios

Six global climate models (GCMs) run under the recent Intergovernmental Panel on Climate Change (IPCC) Fourth Assessment (IPCC 2007) using SRESA2 (A2) and SRESB1 (B1) emission scenarios were employed to assess climate changes and their impacts for the San Francisco Bay region. For this assessment, six models were selected:

- the National Center for Atmospheric Research (NCAR) Parallel Climate Model (PCM),
- the National Oceanic and Atmospheric Administration (NOAA) Geophysical Fluids Dynamics Laboratory (GFDL) model, version 2.1,
- the French Centre National de Recherches Météorologiques CNRM3 model,
- the NCAR CCSM3 model,
- the German MPI ECHAM5 model, and
- the Japanese MIROC3.2 (medium-resolution) model.

These models were selected on the basis of their ability to produce a reasonable representation, from their historical simulation, of the following elements: seasonal precipitation and temperature, the variability of annual precipitation, and the El Niño/Southern Oscillation.

Two greenhouse gas emissions scenarios were considered. The SRES A2, medium-high emission rate represents a differentiated world in which economic growth is uneven and the income gap remains large between now-industrialized and developing parts of the world. People, ideas, and capital are less mobile, so that technology diffuses more slowly. The lower emissions rate SRES B1 emissions scenario presents a future with a high level of environmental and social consciousness, combined with a globally coherent approach to more sustainable development (Figure 1).

The models and scenarios were also required to be ones included in the subset of models that were being used for the 2008 California Climate Change Scenarios Assessment. The general trend is that all of the six simulations warm over the course of the twenty-first century.

Global Atmospheric CO₂ Concentration (ppmv) and Carbon Emissions (GtC)

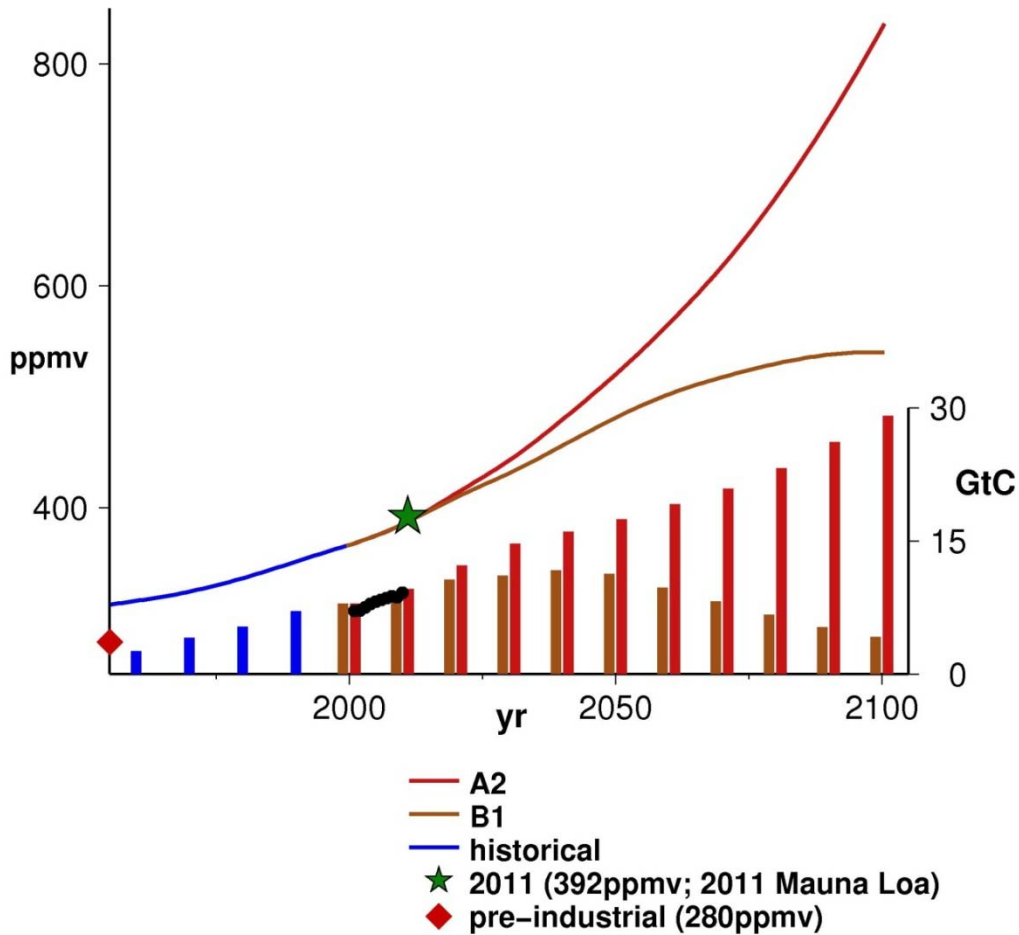


Figure 1: Observed and Projected Carbon Emissions and Annual Global Atmospheric Carbon Dioxide (CO₂) Concentration. Emissions (GtC; gigatons of carbon; 1 GtC corresponds to ~3.67 Gt CO₂) are shown by bars and dots, according to the scale on the right-hand vertical axis. Recent emissions estimates for 2000–2010 are shown by black dots (Carbon Dioxide Information Analysis Center, CDIAC). Historical (observed) emissions are from fossil-fuel burning, cement manufacture, and gas flaring. Carbon dioxide emissions are shown for historical observations (blue bars) and projected periods for B1 (brown bars) and A2 (red bars) emissions scenarios. The annual global atmospheric CO₂ concentration (in parts per million by volume, ppmv) is shown for the period of observations from 1961 to 2000 (blue line), and for the twenty-first century under two emission scenarios: B1 (brown line) and A2 (red line).

Source: The recent CO₂ emissions and concentrations are from CDIAC http://cdiac.ornl.gov/ftp/ndp030/global.1751_2008.ems; Mauna Loa CO₂ from http://scrippsco2.ucsd.edu/data/in_situ_co2/monthly_mlo.csv; projected CO₂ emissions and concentrations from IPCC 2007

Because there is considerable uncertainty in future greenhouse gas emissions, it is not possible to assign odds to either of the two emissions scenarios. The two scenarios are quite similar during the first two decades of the twenty-first century and are consistent with emissions estimated from observations during the recent decade (Figure 1). Importantly, GCMs differ, to

some extent, in their representation of various physical processes from other GCMs, and so the different models contain different levels of warming, different patterns and changes of precipitation, and contain other key differences. The result is a set of model simulations having different climate characteristics, even when the models are driven by the same GHG emissions scenario.

Consequently, the climate projections should be viewed as a set of possible outcomes, with each having an unspecified degree of uncertainty. In short, these models results provide a somewhat fuzzy set of scenarios from which to view the future; they are not detailed predictions. Also, it is important to recognize that the effects of greenhouse gas (GHG) accumulations on climate are somewhat slow to develop and also are long-lasting (IPCC 2007; Hansen 2005; Meehl et al. 2005). Because of this, the levels of warming, the amount of sea-level rise, and other impacts will probably not reach their peaks by 2050. And, as will be seen, results of different mitigation strategies, as expressed by the two GHG emission scenarios (A2: medium-high emissions, and B1: moderately-low emissions) do not become very clear at the 2050 horizon; they are much more distinctly evident in the following decades (IPCC 2007; Hayhoe et al. 2004; Cayan et al. 2008a).

The global climate model temperature was downscaled from the relatively coarse gridding (cells of 100–20 kilometers [km] on a side) to 12 km regional scale gridding using a statistical technique called Bias Correction/Spatial Downscaling (BCSD) (Maurer et al. 2010), superimposed over the San Francisco Bay study domain, as shown in Figure 2.

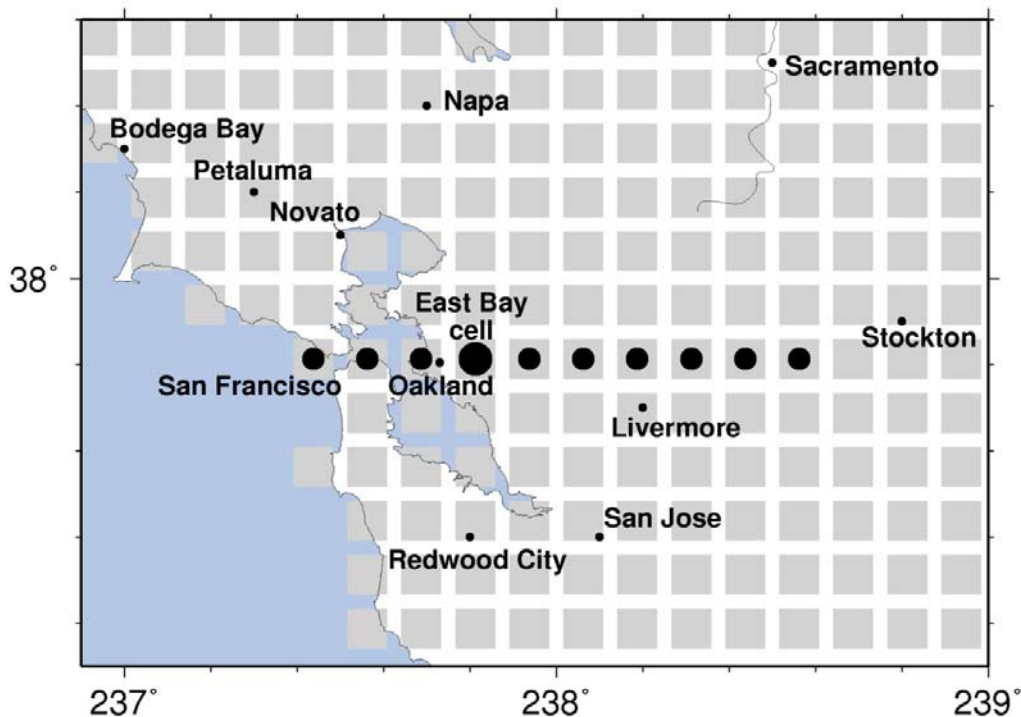


Figure 2: The San Francisco Bay Region, with 12 km Downscaled Grid Superimposed. Black dots show the coast-inland transect, and the large black dot indicates the East Bay grid cell that is used in some of the analyses.

Source: Maurer et al. 2010

Section 2: Warming

Historically, air temperatures over the western United States, including California, appear to have risen significantly over the last several decades (Bonfils et al. 2007). However, quantifying how much warming has occurred across the San Francisco Bay region is problematic because of the subset of weather stations that have existed for many decades. There are few (if any) that have not been contaminated by station moves and/or changes in the immediate surroundings at the station. Almost all of the stations have stronger increases in minimum (nighttime) temperatures than daytime temperatures, in agreement with several previous studies of recent warming over the region and other areas of the globe (Bonfils et al. 2007; Knowles et al. 2006, IPCC 2007; Gershunov et al. 2009; Lebassi et al. 2009).

Besides containing secular changes over several decades, the annual temperature record at San Francisco and surrounding San Francisco Bay locations also exhibit shorter period variability from time scales of a few years to a few decades. From the observed and from the model historical simulations, it is seen that the model simulations begin to warm more substantially in the 1970s; this is likely a response to effects of GHG increases which began to increase significantly during this time period (Bonfils et al. 2007; Barnett et al. 2008).

All of the climate model simulations exhibit warming, globally and regionally over the San Francisco Bay area (Figure 3). Through the first five decades of the twenty-first century, the amount of warming produced by the A2 scenario is nearly the same as that of the B1 scenario, with annual temperatures rising approximately 1.5°C (2.7°F) (Figure 3). But after 2050, the temperatures in the A2 scenario simulations rise faster than those for the B1 scenario simulations.

By the end of the twenty-first century, the envelope of warming in the models' projections, as an annual average, ranges from about 2°C to 6°C (about 3.5 °F to 11°F), and the ensemble mean annual temperature of the A2 scenarios is about 1.5°C greater than that of the B1 scenario, consistent with global scale results (IPCC 2007; Hansen 2005; Meehl et al. 2005). The rate of warming, especially in the latter half of the twenty-first century, is considerably greater than warming rates from global and regional estimates from observed historical data (e.g., IPCC 2007; Bonfils et al. 2007). The individual model simulations contain year-to-year and decade-to-decade variability that is superimposed upon the overall greenhouse gas warming over the twenty-first century (Figure 3). Also, there is considerable asymmetry in the amount of warming, both seasonally (Figure 4) and spatially (Figure 5). Importantly, as in several of the climate model simulations (IPCC 2007; Cayan et al. 2008a) there is greater warming in summer than in winter (Figure 4).

During summer, the models suggest that climate warming of land surface temperatures over the San Francisco Bay region becomes greater at locations that are distant from the coast (Figure 5). In both the B1 and A2 emission scenario simulations, there is a distinct Pacific Ocean influence, wherein warming is more moderate in the coastal zone, near San Francisco, but rises considerably, by almost 1°C (1.8°F) higher, in the interior landward area, near Stockton. There is considerable variability between the six GCMs, with the lower-sensitivity models such as PCM exhibiting the lowest temperature rise in both cool and warm seasons, and vice versa for higher sensitivity models such as GFDL.

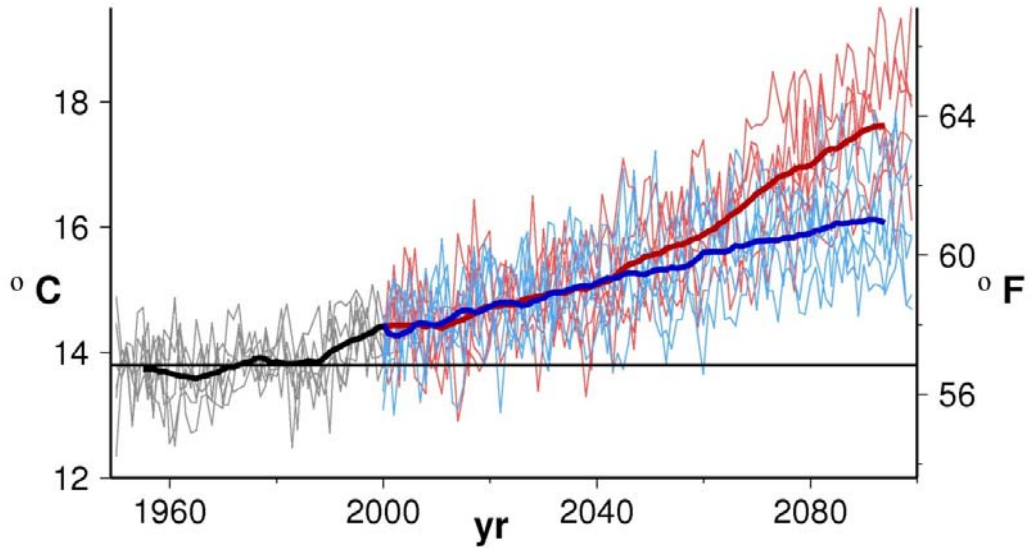


Figure 3: Annual Temperature (°C left; °F right) Simulated for Historical and Future Periods for the East Bay Grid Cell Using BCSD Downscaling of Six GCMs (CNRM CM3, GFDL CM2.1, MIROC3.2med, MPI ECHAM5, NCAR CCSM3, and NCAR PCM1). Thin grey lines show simulated historical values (1950–1999). Thin blue and red lines show values from B1 and A2 simulations (2000–2099). Thick lines show 11-year running mean smoothed median of historical (black), B1 (blue), and A2 (red) simulations. Horizontal black line shows average of the six GCM’s over the historical (1961–1990) period.

Source: GCMs from PCMDI www-pcmdi.llnl.gov/; downscaling as in Maurer and Hidalgo 2008

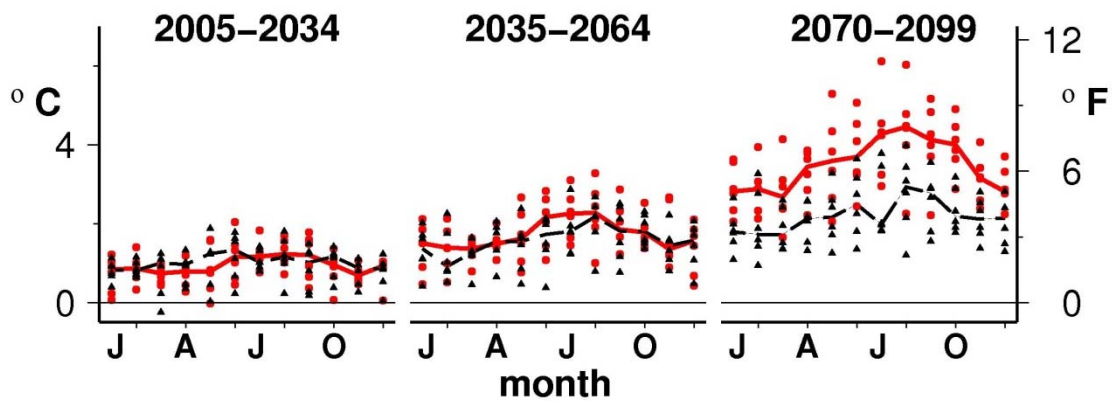


Figure 4: Monthly BCSD Simulated Temperature Changes (°C left; °F right) for the East Bay Grid Cell for Six GCMs. Changes (from 1961–1990) are shown for three time periods: early century (2005–2034; left), mid-century (2035–2064; middle) and late century (2070–2099; right). Changes are shown in each panel for January (left) to December (right). Black and red symbols show changes for B1 and A2 emission scenarios, respectively. Black (dashed; B1) and red (solid; A2) lines show the median value for each of the six models. GCMs used are those listed in Figure 3.

Source: GCMs from PCMDI www-pcmdi.llnl.gov/; downscaling as in Maurer and Hidalgo 2008.

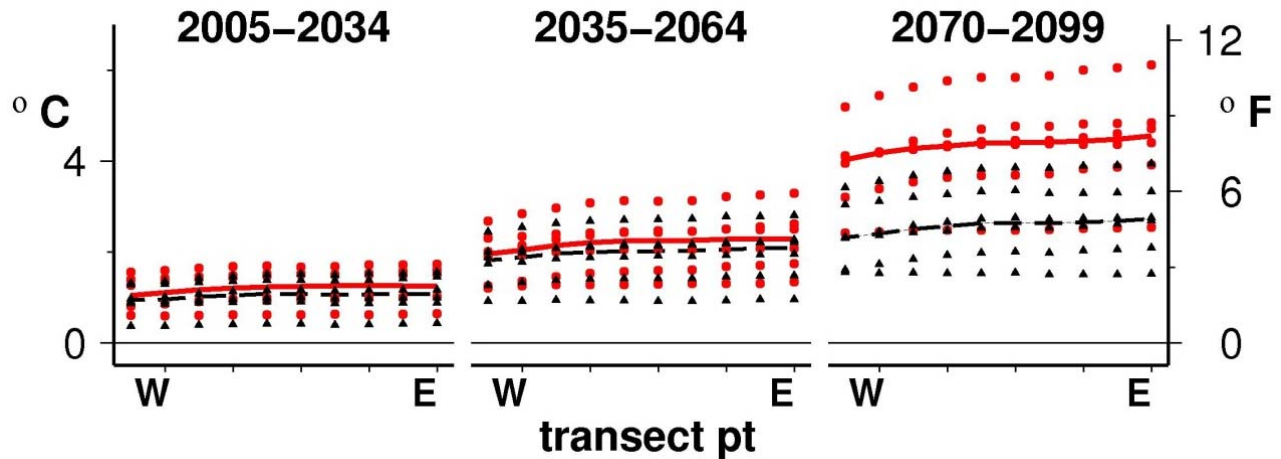


Figure 5: July–September BCS D Surface Air Temperature Changes (°C left; °F right) Over the Coast-to-Inland Transect (see Figure 1). Changes (from 1961–1990) are shown for three time periods: early century (2005–2034; left), mid-century (2035–2064; middle) and late century (2070–2099; right). Changes are shown in each panel over the transect line from west (right) to east (left). Black and red symbols show changes for B1 and A2 emission scenarios, respectively. Black (dashed; B1) and red (solid; A2) lines show the median value for the six models. GCMs used are those listed in Figure 3.

Source: GCMs from PCMDI www.pcmdi.llnl.gov/; downscaling as in Maurer and Hidalgo 2008.

Historically, extreme warm temperatures in the San Francisco Bay region have mostly occurred in July and August, but as climate warming takes hold, the occurrences of these events will likely begin in June and could continue to occur in September (Figure 6). All simulations indicate that hot daytime and nighttime temperatures (heat waves) increase in frequency, magnitude, and duration from the historical period and during the projected period through the first half of the twenty-first century. As shown in Figure 6, for a location over the interior portion of San Francisco Bay, region simulations exhibit an increase of more than threefold in frequency and a decided increase in intensity of hot days. Within a given heat wave, there is an increasing tendency for multiple hot days in succession—heat waves last longer.

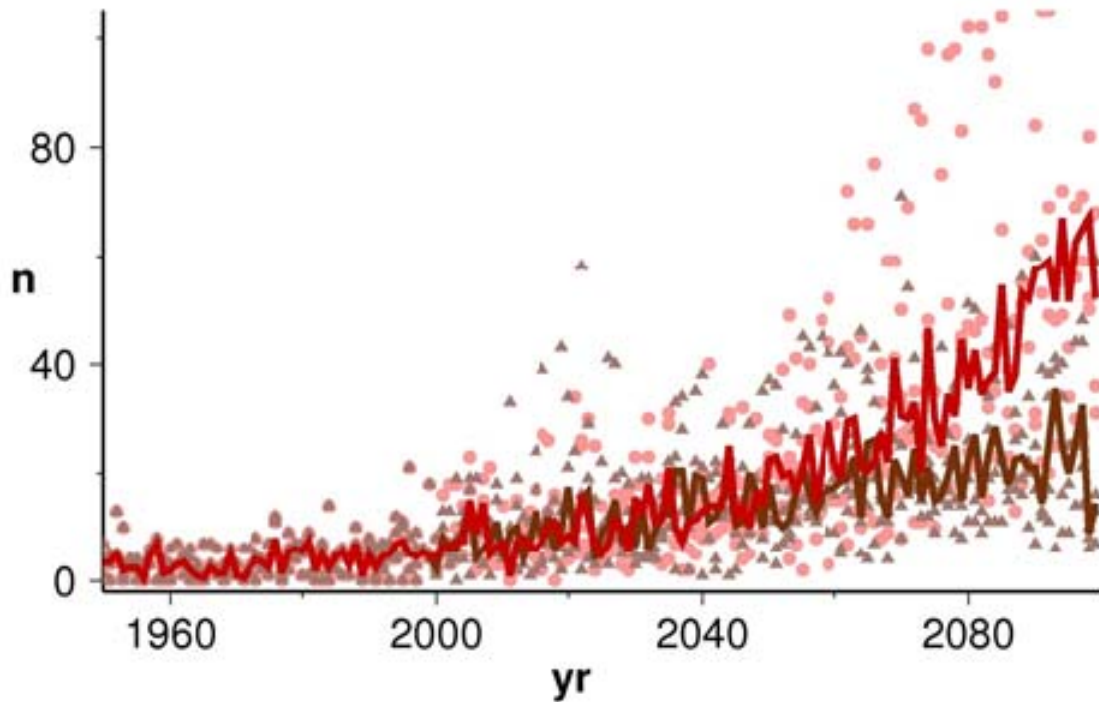


Figure 6: Number of Days (n), April–October, When Maximum Temperature (Tmax) Exceeds the 98th Percentile Historical (1961–1990) Level of 28°C (82.4°F) for the East Bay Grid Cell from Four Bias-Corrected/Constructed Analogs (BCCA) Downscaled GCMs. Brown carrots and red dots represent the B1 and A2 emission scenarios, respectively. Thick brown (B1) and red (A2) lines show the median value from the four simulations.

Source: GCMs from PCMDI www.pcmdi.llnl.gov/; downscaling as in Maurer et al. 2010.

Section 3: Precipitation

Precipitation in the San Francisco Bay region is characterized by a strong Mediterranean pattern wherein most of the annual precipitation falls in the cooler part of the year between November and March. The climate change simulations from these GCMs indicate that the San Francisco Bay region will retain its Mediterranean climate, with relatively cool and wet winters and hot dry summers, as evidenced by the individual strands in the ensemble of downscaled projections (Figure 7). The simulations indicate that the high degree of variability of annual precipitation will also prevail during the next five decades, which would suggest that the region will remain vulnerable to drought.

Annual (water year) precipitation changes, for each decade of the first half of the twenty-first century, as taken from the three GCMs for the A2 and the B1 emission scenarios, produce mixed results. However, some (the majority of simulations considered here) become drier than the historical annual average during the middle and end of the twenty-first century. The lack of consistency between models is also seen in a larger sample of model simulations (not shown), and underscores the caution that should be placed in the interpretation of these results – the possible changes in annual precipitation are quite uncertain. The differences between models is partly a result of the high variability in yearly precipitation compared to any longer-term trend, and is in keeping with California’s historical behavior being marked by considerable precipitation variability between years and decades. Nonetheless, considering simulated precipitation changes at the monthly level, the decline in annual precipitation indicates that the greatest reduction in precipitation occurs in March and April, while the core winter months are relatively unchanged (see also Pierce et al. 2012) (Figure 8).

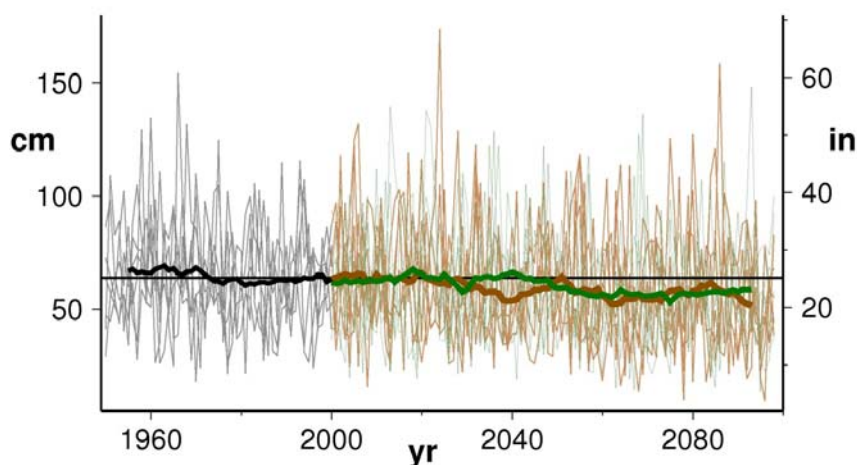


Figure 7: Simulated Annual Precipitation (cm right; inches left) at an East Bay Grid Cell from Six GCMs for Historical and Projected Twenty-First Century B1 and A2 Emission Scenarios. The thin black line shows the individual GCM precipitation simulated for 1950–1999. Thin green lines and brown lines show values from B1 and A2 simulations, respectively. Thick lines show 11-year running mean smoothed median of the six historical (black), B1 (green), and A2 (brown) simulations. The GCMs used are those listed in Figure 3.

Source: GCMs from PCMDI www-pcmdi.llnl.gov/.

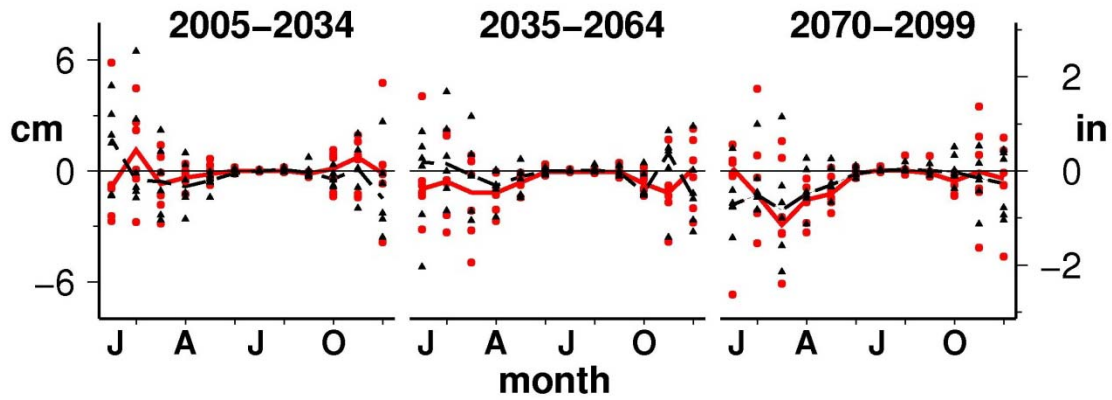


Figure 8: Precipitation Changes (cm right; inches left) for Each Month of the Year, from Six GCMs for the East Bay Grid Cell. Changes (from 1961–1990) are shown for three time periods: early century (2005–2034; left), mid-century (2035–2064; middle) and late century (2070–2099; right). Changes are shown in each panel for January (left) to December (right). Black and red symbols show changes for B1 and A2 emission scenarios, respectively. Black (dashed; B1) and red (solid; A2) lines show the median value for the six models. The GCMs used are those listed in Figure 3.

Source: GCMs from PCMDI www-pcmdi.llnl.gov/.

Section 4: Sea-Level Rise

Over the past several decades of tide gage observations, sea level measured along the California coast from San Francisco southward to La Jolla has risen at a rate of about 17–20 cm (7–8 in) per century. In the future, as climate warms, it is quite possible that the rate of sea-level rise will increase due to enhanced ocean thermal expansion and increased melting of ground-based ice, especially in Greenland and Antarctica. Semi-empirical methods (Rahmstorf 2010) operate on the premise that global sea-level rise can be linked to large-scale measures of global mean surface air temperature, which is evident from historical observed and proxy data over more than one century of records. The semi-empirical technique provides a methodology to estimate global sea level using the surface air temperature projected by the global climate model simulations, and leads to larger rates of sea-level rise than were produced by other recent estimates (IPCC 2007; Cayan et al. 2008b).

The present estimates assume that sea-level rise along the California coast, in particular at the mouth of San Francisco Bay, will be the same as the global estimates. The present assessment employed the Vermeer and Rahmstorf (2009) method for estimating sea-level rise, a modification of the semi-empirical method introduced by Rahmstorf (2007), using global surface air temperature to derive one set of sea-level projections. The resulting estimates (Figure 9) indicate that potential sea-level rise over the next five decades will increase over its historical rate by a considerable amount. By 2050, sea-level rise, relative to the 2000 level, ranges from approximately 27 to 48 cm (11 to 19 in), and by 2100 sea-level rise ranges from approximately 77 to 140 cm (30 to 55 in).

To investigate sea-level extremes, a model was constructed to investigate future sea level at the San Francisco tide gage location. The model included astronomical tides, surface pressure and wind effects, El Niño/Southern Oscillation (ENSO) influence, and the secular change from global sea-level rise provided by the Vermeer and Rahmstorf (2009) scheme. With these components, simulated sea level at San Francisco was constructed by superimposing the sea-level rise onto predicted tides, weather-related sea-level anomalies, and ENSO-related sea-level fluctuations. The result of the model runs was a series of hourly sea level from 1950 through 2100, corresponding to each of the four climate simulations. As sea-level rises, there will be an increased rate of extreme high sea-level events, which increases the duration of extremely high water (Figure 10). This increases the exposure to potential damage, since the winter storms that result in anomalously high sea levels are often accompanied by high winds and high ocean waves (Cayan et al. 2008b). Importantly, as sea level rises over the next several decades, there would be an increasing tendency for heightened sea-level events to persist for more hours, as illustrated in Figure 10, which would likely result in a greater threat of coastal erosion and other damage.

sea level projections

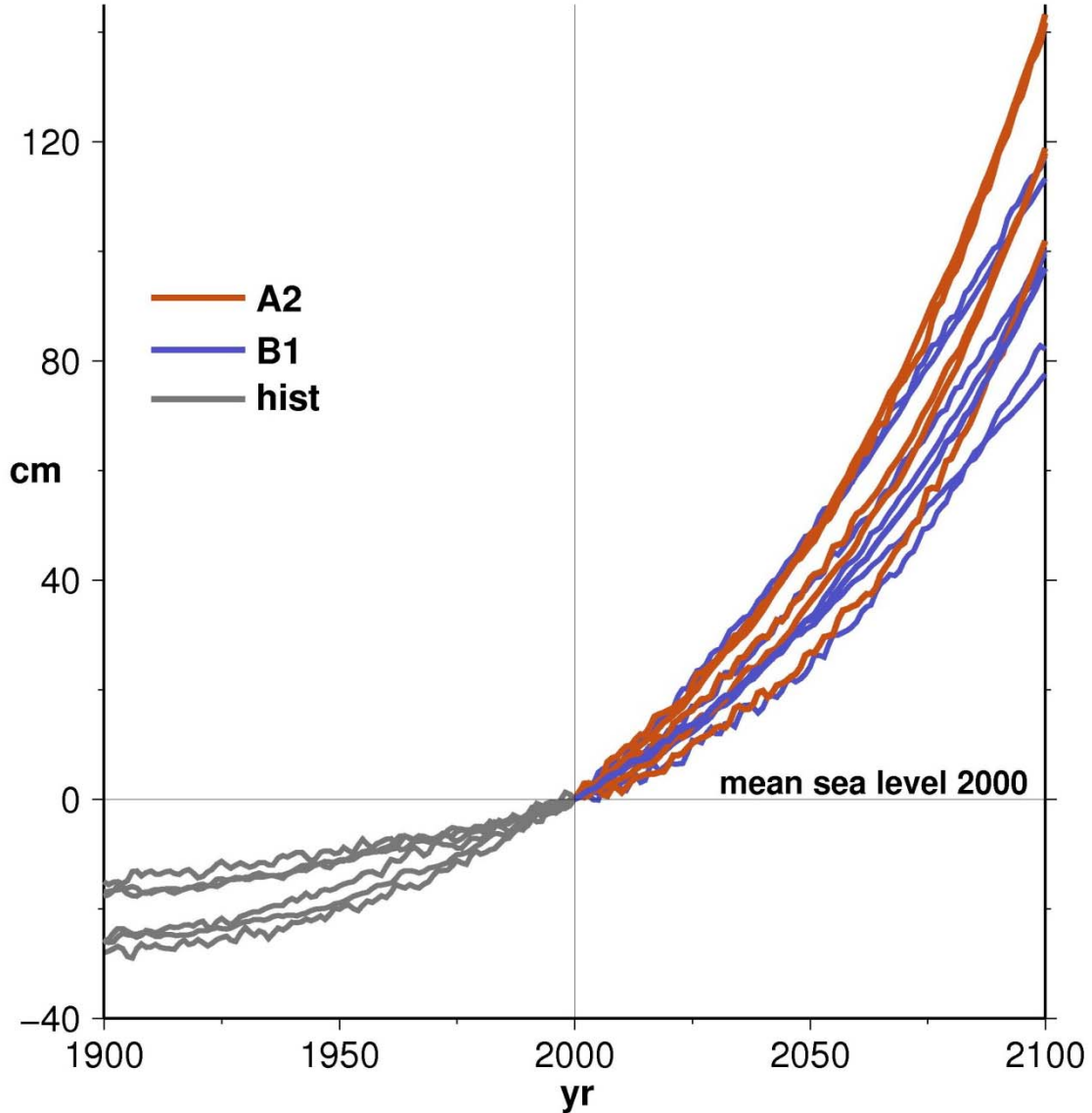


Figure 9: Sea Level (cm) Projections Using the Vermeer and Rahmstorf (2009) Semi-Empirical Scheme. The Vermeer and Rahmstorf (2009) scheme is developed to estimate global mean sea level, but there is general agreement between estimated global sea level and the multi-decade trend of historical observations along the California coast from San Francisco southward to San Diego. The thin black line indicates mean sea level for 2000. Grey lines show global sea-level estimates during the period before 2000 (historical simulation). Sea-level estimates for 2000–2100 are shown using projections from two emissions scenarios: A2 (red) and B1 (blue). Over the twentieth century, sea-level records along the California coast have quite closely mirrored the global rate of sea-level rise. The GCMs used are those listed in Figure 3.

Source: GCMs from PCMDI www-pcmdi.llnl.gov/; sea level rise method is that of Vermeer and Rahmstorf 2009.

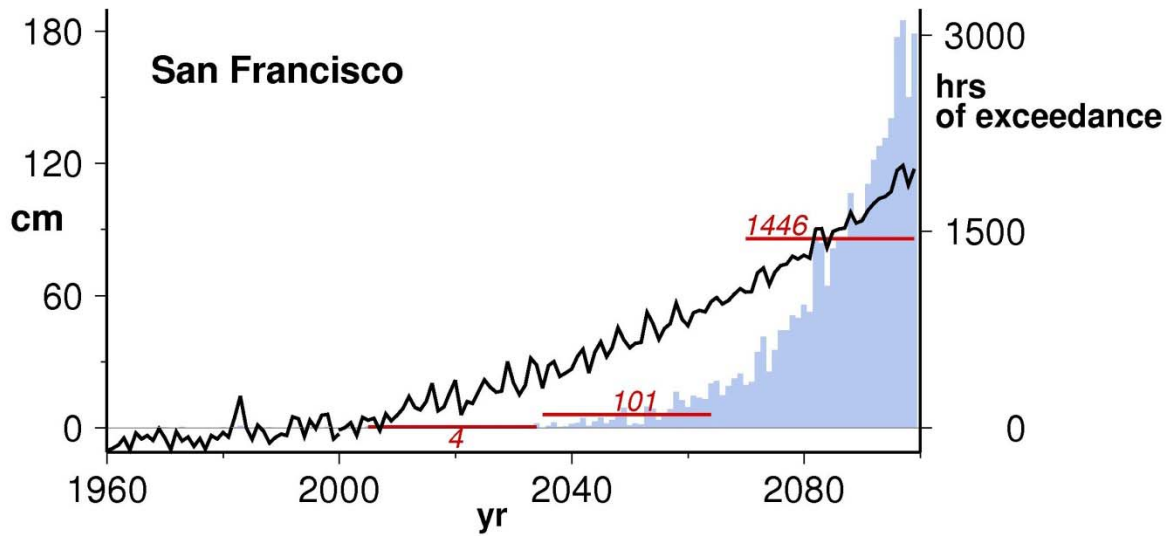


Figure 10: Sea-Level Rise and Hours of Extreme Sea Level Projected for San Francisco. The figure shows the annual sea level (cm; black line) and total hours above the historical 99.99th percentile sea level (blue bars) from observations and from sea-level hourly model computations using the GFDL CM2.1 simulation for the A2 emissions scenario as a representative example. The average number of hours which the projected sea level was found to exceed the historical 99.99th percentile are shown in red for the periods 2005–2034, 2035–2064, and 2070–2099. The projected sea-level rise (secular trend) is based on the GFDL model air temperature and the Vermeer and Rahmstorf 2009 sea-level rise scheme.

Source: GCMs from PCMDI www-pcmdi.llnl.gov/; sea level rise method is that of Vermeer and Rahmstorf 2009. Hourly sea level projection adopted from Cayan et al. 2008b.

References

- Barnett, T. P. et al. 2008: "Human-Induced Changes in the Hydrology of the Western United States." *Science* 319 (5866): 1080–1083. DOI: 10.1126/science.1152538.
- Bonfils, C., P. B. Duffy, B. D. Santer, D. B. Lobell, T. J. Phillips, T. M. L. Wigley, and C. Doutriaux. 2007: Detection of unusual temperature trends in California. *Climatic Change*.
- Cayan, D. R., E. P. Maurer, M. D. Dettinger, M. Tyree, and K. Hayhoe. 2008a: "Climate change scenarios for the California Region." *Climatic Change* 87 (Suppl 1):S21-S42. DOI 10.1107/s10584-007-9377-6.
- Cayan, D. R., P. D. Bromirski, K. Hayhoe, M. Tyree, M. D. Dettinger, and R. E. Flick. 2008b: "Climate change projections of sea level extremes along the California Coast." *Climatic Change* 87 (Suppl 1): S57–S73. DOI 10.1007/s10584-007-9376-7.
- Gershunov, A., T. P. Barnett, D. R. Cayan, A. Tubbs, and L. Goddard. 2000: "Predicting ENSO Impacts on Intraseasonal Precipitation Statistics in California: The 1997–1998 Event." *J. of Hydromet.* 1 (6): 201–210.
- Gershunov, A., D. R. Cayan, and S. F. Jacobellis. 2009: "The Great 2006 heat wave over California and Nevada: Signal of an Increasing Trend." *Journal of Climate* Early Online Release. DOI: 10.1175/2009JCLI2465.1.
- Hansen, J. E. 2005: "A slippery slope: How much global warming constitutes 'dangerous anthropogenic interference?' An editorial essay." *Clim. Change* 68: 269–279. doi:10.1007/s10584-005-4135-0.
- Hayhoe, K., D. Cayan, C. B. Field, P. C. Frumhoff, E. P. Maurer, N. L. Miller, S. C. Moser, S. H. Schneider, K. N. Cahill, E. E. Cleland, L. Dale, R. Drapek, R. M. Hanemann, L. S. Kalkstein, J. Lenihan, C. K. Lunch, R. P. Neilson, S. C. Sheridan, and J. H. Verville. 2004: "Emissions pathways, climate change, and impacts on California." *Proc Natl Acad Sci USA*. 2004 Aug 24; 101(34): 12422–7. Epub 2004 Aug 16.
- IPCC. 2007. IPCC Fourth Assessment Working Group I Report "Climate Change 2007 The Physical Science Basis." ISBN 978 0521 88009-1. <http://www.ipcc.ch/ipccreports/ar4-wg1.htm>.
- Knowles, N., M. D. Dettinger, and D. R. Cayan. 2006: "Trends in Snowfall versus Rainfall in the Western United States." *J. Climate* 19 (18): 4545–4559.
- Lebassi B., J. E. González, D. Fabris, C. Milesi, N. L. Miller, P. Switzer, and R. Bornstein. 2009: "Observed 1970–2005 cooling of summer daytime temperatures in coastal California." *J. of Climate* 22: 3558–3573.
- Maurer, E.P., and H.G. Hidalgo, 2008: Utility of daily vs. monthly large-scale climate data: an intercomparison of two statistical downscaling methods, *Hydrology and Earth System Science*, 12, 551-563.
- Maurer, E. P., H. G. Hidalgo, T. Das, M. D. Dettinger, and D. R. Cayan. 2010: "The utility of

daily large-scale climate data in the assessment of climate change impacts on daily streamflow in California." *Hydrol. Earth Syst. Sci.* 14: 1125–1138, doi:10.5194/hess-14-1125-2010. <http://www.hydrol-earth-syst-sci.net/14/1125/2010/hess-14-1125-2010.html>.

Meehl, G. A., W. M. Washington, W. D. Collins, J. M. Arblaster, A. Hu, L. E. Buja, W. G. Strand, and H. Teng. "How much more global warming and sea level rise?" *Science* 2005 Mar 18; 307(5716):1769–72.

Pierce, D. W. et al. 2012: Probabilistic estimates of future changes in California temperature and precipitation using statistical and dynamical downscaling. *Climate Dynamics*, in press.

Rahmstorf, S. 2007: "A Semi-Empirical Approach to Projecting Future Sea-Level Rise." *Science* 315 (5810): 368–370. DOI: 10.1126/science.1135456.

Rahmstorf, S. 2010: "A new view on sea level rise." *Nature Rep Clim Change* 4:44–45.

Vermeer, M., and S. Rahmstorf. 2009: "Global Sea Level Linked to Global Temperature." *Proc Natl Acad Sci USA* 106: 21527–21532.

Glossary

A2	medium-high emissions scenario
B1	lower emissions scenario
BCSD	Bias Correction/Spatial Downscaling
BCCA	Bias-Corrected/Constructed Analogs
CCSM3	NCAR Community Climate System Model Version 3
CDIAC	Carbon Dioxide Information Analysis Center
CNRM	Centre National de Recherches Météorologiques
CO ₂	carbon dioxide
GCM	global climate models
GFDL	Geophysical Fluids Dynamics Laboratory
GHG	greenhouse gas
GtC	gigatons of carbon
IPCC	Intergovernmental Panel on Climate Change
LLNL	Lawrence Livermore National Laboratory
MIROC3.2	A Japanese medium-resolution model
MPI ECHAM5	Max Planck Institute general circulation model
NCAR	National Center for Atmospheric Research
NOAA	National Oceanic and Atmospheric Administration
PCDMI	Program for Climate Model Diagnosis and Intercomparison
PCM	Parallel Climate Model
PIER	Public Interest Energy Research Program
ppmv	parts per million by volume
RISA	Regional Integrated Sciences and Assessments Program
SLR	sea-level rise
SRES	Special Report on Emissions Scenarios